Journal of Experimental Botany, Vol. 67, No. 5 pp. 1477–1492, 2016
doi:10.1093/jxb/erv543 Advance Access publication 28 December 2015

RESEARCH PAPER

Stable methylation of a non-coding RNA gene regulates gene expression in response to abiotic stress in *Populus simonii*

Yuepeng Song[1,2,*], Dong Ci[1,2,*], Min Tian[1,2] and Deqiang Zhang[1,2,†]

[1] National Engineering Laboratory for Tree Breeding, College of Biological Sciences and Technology, Beijing Forestry University, No. 35, Qinghua East Road, Beijing 100083, PR China
[2] Key Laboratory of Genetics and Breeding in Forest Trees and Ornamental Plants, College of Biological Sciences and Technology, Beijing Forestry University, No. 35, Qinghua East Road, Beijing 100083, PR China

* These authors contributed equally to this work.
† Correspondence: DeqiangZhang@bjfu.edu.cn

Received 28 July 2015; Accepted 30 November 2015

Editor: Ramanjulu Sunkar, Oklahoma State University

Abstract

DNA methylation plays important roles in responses to environmental stimuli. However, in perennial plants, the roles of DNA methylation in stress-specific adaptions to different abiotic stresses remain unclear. Here, we present a systematic, comparative analysis of the methylome and gene expression in poplar under cold, osmotic, heat, and salt stress conditions from 3 h to 24 h. Comparison of the stress responses revealed different patterns of cytosine methylation in response to the four abiotic stresses. We isolated and sequenced 1376 stress-specific differentially methylated regions (SDMRs); annotation revealed that these SDMRs represent 1123 genes encoding proteins, 16 miRNA genes, and 17 long non-coding RNA (lncRNA) genes. The SDMR162 region, consisting of Psi-MIR396e and PsiLNCRNA00268512, is regulated by epigenetic pathways and we speculate that PsiLNCRNA00268512 regulates miR396e levels by acting as a target mimic. The ratios of methylated cytosine declined to ~35.1% after 1 month of recovery from abiotic stress and to ~15.3% after 6 months. Among methylated miRNA genes, only expression of the methylation-regulated gene *MIRNA6445a* showed long-term stability. Our data provide a strong basis for future work and improve our understanding of the effect of epigenetic regulation of non-coding RNA expression, which will enable in-depth functional analysis.

Key words: DNA methylation, abiotic stress, non-coding RNA, *Populus simonii*, transcriptome changes.

Introduction

DNA methylation plays important roles in transposon silencing, heterochromatin organization, genomic imprinting, and gene expression (Zhang *et al.*, 2006; Suzuki and Bird, 2008). In plants, four classes of DNA methyltransferases methylate cytosines in three different contexts, CG, CHG, and CHH (H=A, C, or T) (Chan *et al.*, 2005). DNA methylation patterns also respond to stress; for example, the tobacco *NtGPDL* gene was demethylated at CCGG sites within 1 h under aluminum stress (Choi and Sano, 2007) and genome-wide demethylation occurred in root tissues of maize seedlings exposed to cold stress (Steward *et al.*, 2002). In contrast, global genome methylation and homologous recombination frequency increased in Arabidopsis exposed to salt, UV-C, cold, heat, or flood stress (Boyko *et al.*, 2010). Under salt

stress, hypermethylation of CCWGG sequences and satellite DNA is associated with a switch from C_3 photosynthesis to the Crassulacean acid metabolism pathway of carbon dioxide assimilation in *Mesembryanthemum crystallinum* (Dyachenko *et al.*, 2006). Single base resolution methylomes of *Populus trichocarpa* reveal increased levels of methylated cytosines under drought stress (Liang *et al.*, 2014). All these studies showed that DNA methylation in response to abiotic stress occurs commonly in plants, but the response patterns might differ significantly in different species.

In contrast to annual plants, perennial plants must adapt to simultaneous and/or seasonal exposure to various abiotic stresses, which can affect their growth and survival. DNA methylation plays important roles in genomic responses to environmental stimuli; however, the DNA methylation patterns for stress-specific adaption in response to different abiotic stresses remain unclear in perennial plants. However, one study showed that levels of methylated cytosines, including 2 kb upstream and downstream of transcription start sites, and in repetitive sequences, significantly increased after drought treatment in *Populus*, suggesting that loci responsive to DNA methylation might show a biased distribution in the genome (Liang *et al.*, 2014).

Previous studies have focused on cytosine methylation of genic regions (Vining *et al.*, 2012; Lafon-Placette *et al.*, 2013), but the regulatory relationship between methylation and elements of intergenic regions remains poorly explored. However, increasing evidence indicates that expression of miRNA genes is also regulated by epigenetic modification. MiRNAs, transcribed from loci in the intergenic regions of the genome, negatively regulate gene expression at the transcriptional and/or post-transcriptional levels by degrading or inhibiting the translation of target mRNAs (Carthew and Sontheimer, 2009; Voinnet, 2009; Chen, 2010). Song *et al.* (2015) found that ~28% of miRNA genes (113 miRNA genes) were methylated in bisexual flower development in andromonoecious poplar. Also, in human cells, repression of miRNA genes is closely associated with hypermethylation of their promoter regions in cancer cells (Li *et al.*, 2011). Intergenic regions also encode long non-coding RNAs (lncRNAs), non-coding RNA transcripts of >200 nucleotides in length (Kapranov *et al.* 2007), and recent studies have shown that lncRNAs play important roles in the regulation of flowering, male sterility, metabolism, and biotic and abiotic stress responses (Zhang *et al.*, 2013). LncRNAs can be processed to small RNAs and interact with other classes of non-coding RNAs (Jalali *et al.*, 2012, 2013). Described as the 'dark matter' of the genome (van Bakel *et al.*, 2010), the methylation of lncRNA genes is still rarely annotated.

Epigenetic regulation has important effects on the responses to abiotic stress, and studies indicate that stress-responsive changes under epigenetic regulation can persist over long periods or even be inherited over successive generations (Molinier *et al.*, 2006). Global methylation levels of *ZmMI1* analyzed using HPLC showed that methylation levels declined from 38.4% to 24.7% after 5 d of chilling stress and declined further to 22.5% after samples were returned to 23 °C and cultivated for an additional 7 d (Steward *et al.*, 2002). In contrast, in potato, >60% of methylated loci detected in the parents were also detected in all six generations of self-bred progeny (Nakamura and Hosaka, 2010). Increased global genome methylation of Arabidopsis in response to various abiotic stresses enhances the stress tolerance of untreated progeny (Boyko *et al.*, 2010). In plants with limited seed dispersal or asexual reproduction, most individuals will probably experience similar growth conditions to their (maternal) parents. These long-term and transgenerational effects of stress-responsive DNA methylation might play important roles in adaptation to complex environmental conditions in the progeny. However, the stability of stress-responsive methylation in perennial plants is still unknown.

Given the increasing evidence for the involvement of DNA methylation in responses to abiotic stress, together with the role of methylation in regulating gene expression, we hypothesized that DNA methylation changes would occur in plants exposed to different abiotic stresses and play important roles in stress-responsive gene expression. We present here a systematic comparative methylome and miRNA sequencing analysis in poplar under four abiotic stress conditions: salinity, osmotic, heat, and cold stress. *Populus simonii* shows distinctive expression patterns of genes related to photosynthesis, hormone signaling, phytohormone biosynthesis, and antioxidant enzyme systems under abiotic stress and high tolerance to stress (Song *et al.*, 2014). Thus, we use this adaptable and resistant species (Wei *et al.*, 2012) for MSAP [methylation-sensitive amplified fragment length polymorphism (AFLP)] and miRNA sequencing analysis, which revealed distinct DNA methylation and gene expression patterns in response to these stresses. This work provides a new picture of poplar epigenetic regulation mechanisms in response to different abiotic stresses.

Materials and methods

Plant materials and treatments

The annual *P. simonii* 'QL9', a stress-tolerant genotype (see Supplementary Methods S1 available at *JXB* online), was planted in pots under natural light conditions (1250 μmol m^{-2} s^{-1} of photosynthetically active radiation), 25 ± 1 °C (day and night), 50 ± 1% relative humidity (day and night), and a 12 h day/night regime in an air-conditioned greenhouse using soilless culture technology. Sixty annual clones of the same size (50 cm in height) were used in this study. These clones were divided into five groups of 12 clones. These groups were exposed to 150 mM NaCl, 30% polyethylene glycol (PEG) 6000, 42 °C, and 4 °C for 3, 6, 12, and 24 h for salinity, osmotic, heat, and cold stress treatments, respectively. The 3 h and 6 h time points were chosen to capture early responsive genes, and the 24 h time point for late responsive genes (Lee *et al.*, 2005). After 24 h, abiotic stress treatments were removed from all sample groups to detect long-term changes of DNA methylation and gene expression. For the 1 and 2 month time points, treated leaves were used for analysis of methylation stability. After 6 months, newly emerged leaves after dormancy were selected for analysis of methylation stability. Clones not exposed to abiotic stress were used as the control group. Three biological replicates were used for each treatment time point, including the control group. For physiological and gene

expression analysis, fresh leaves were collected from the five groups, then immediately frozen in liquid nitrogen and stored at –80 °C until analysis.

HPLC analysis of DNA methylation levels

DNA methylation levels were measured by HPLC according to the method of Wang *et al.* (2002). Methylcytosine and cytosine were measured by HPLC according to the method of Demeulemeester *et al.* (1999), where w represents the content of related cytosine. The percentage of DNA methylation was determined by the formula below:

$$\text{Percentage}(\%) = \frac{w(5-\text{methylcytosine})}{w(5-\text{methylcytosine}) + w(5-\text{cytosine})}$$

Methylation-sensitive AFLP (MSAP) analysis

MSAP analysis was carried out based on an established protocol (Sha *et al.*, 2005; Peredo *et al.*, 2006), and the isoschizomers *Hpa*II and *Msp*I were employed as 'frequent-cutter' enzymes. During the selective PCR step, *Eco*RI and *Hpa*II/*Msp*I primers with three additional selective nucleotides were used. The selective PCR products were resolved by electrophoresis on 6% sequencing gels and detected with silver staining (Tixier *et al.*, 1997). The differentially amplified fragments represent stress-responsive differentially methylated regions.

The procedure for isolating polymorphic bands was performed as described previously (Sha *et al.*, 2005). Briefly, polymorphic fragments were excised from the gels, hydrated in 50 µl of water, and incubated at 42 °C for 30 min. The eluted DNA was amplified with the same primer pairs and under the same conditions used for selective amplification. Sequence information was obtained by cloning the fragments into the pMD18-T vector (Takara Bio Inc., Tokyo, Japan), and three positive clones for each individual were selected for sequencing. The sequences were analyzed using JGI BLAST algorithms (http://www.phytozome.net) (Altschul *et al.*, 1990) and NCBI BLAST algorithms (http://www.ncbi.nlm.nih.gov) (Johnson *et al.*, 2008).

Sequencing of candidate methylated regions

To verify DNA methylation sites derived from MSAP analysis, we designed primers specific for methylated and unmethylated bisulfite-treated DNA using Methyl Primer Express (v1.0) software (Herman *et al.*, 1996). The assay primers span a region that contains the 5′-CCGG-3′ sites. MSP reactions were performed using bisulfite-treated DNA as templates, and were carried out for 25 cycles. Primer sequences and annealing temperatures are listed in Supplementary Table S1. Sequence information was obtained by cloning the fragments into the pMD18-T vector (Takara Bio Inc.), and 15 positive clones for each individual were selected for sequencing. All sequencing was performed on the three replicates.

Transcriptome analysis

The RNeasy Plant mini kit (Qiagen, Hilden, Germany) and SuperScript First-Strand Synthesis system (Invitrogen) were used for total RNA extraction and cDNA synthesis, respectively. The experiments were conducted as described by Song *et al.* (2014) (Supplementary Methods S1). To identify differentially expressed genes, miRNAs, and lncRNAs under salinity, osmotic, heat, and cold stress, we used the 6 h treatment group for transcriptome analysis including microarray analysis, miRNA sequencing, and lncRNA sequencing. Fresh leaf tissue samples were collected from the three independent biological replicates for RNA extraction. Amplification, labeling, purification, and hybridization were performed at the Shanghai Bio Institute. The detailed gene expression analysis process is available in Supplementary Method S1. The RNA–RNA interaction was predicted independently, based on the minimum free energy structure of RNA–RNA interaction using RNAplex (Tafer and Hofacker, 2008).

5′-RACE

RNA ligase-mediated 5′-rapid amplification of cDNA ends (RLM-RACE) was performed with the First Choice RLM-RACE Kit (Ambion, Austin, TX, USA), as described by Song *et al.* (2015). PCR was performed with 5′ adaptor primers and 3′ gene-specific primers using cDNA as the template (see Supplementary Table S2). The RACE products were gel-purified, cloned, and sequenced.

Quantitative real-time PCR

For analysis of the expression of protein-coding and non-coding RNA genes, a TaKaRa ExTaq R PCR Kit, SYBR green dye (TaKaRa, Dalian, China), and a DNA Engine Opticon 2 machine (MJ Research) were used. Gene-specific primers were designed to target the 3′-untranslated region (UTR) of each gene (Supplementary Table S3). A melting curve was used to check the specificity of each amplified fragment. For all reactions, triplicate technical and biological repetitions of each individual were performed. The PCR was performed according to Song *et al.* (2014). After amplification, the PCR products were sequenced to check the specificity of the primer sets. Relative expression levels of candidate genes were standardized to the transcript levels for *PsiACTIN*, which shows stable expression under abiotic stress, calculated by the $2^{-\Delta\Delta}$Ct method (Livak and Schmittgen, 2001). Relative expression levels of non-coding RNAs were standardized to the transcript levels for 5.8S rRNA. To validate the correlation of miRNA and target expression, improved degradome sequencing libraries were used to detect cleaved transcripts of targets. The details of these libraries are shown in Supplementary Fig. S1.

Data analysis

For cluster analysis and display of genome-wide differentially methylated sites, the Cluster and Tree View software packages were used for average linkage hierarchical clustering (Eisen *et al.*, 1998). For statistical analysis of differentially expressed genes, one-way ANOVA was performed using R software. Significant differences between different stress treatments were determined through LSD test. Differences were considered statistically significant when $P<0.05$.

Data access

The gene expression data reported here are available from NCBI with the GEO accession numbers SRP060590, GSE43872, GSE42530, GSE37608, and GSE41557.

Results

Global DNA methylation activates responses to abiotic stress

To examine how DNA methylation changes in response to abiotic stress, we used HPLC to measure the dynamic cytosine methylation levels of the *P. simonii* genome over a time course of salinity, osmotic, heat, and cold stress treatment (0, 3, 6, 12, and 24 h) (Fig. 1). Cytosine methylation levels significantly increased after 3 h of treatment for all four abiotic stresses (Fig. 1A). Heat stress induced significantly higher cytosine methylation levels than the other abiotic stresses,

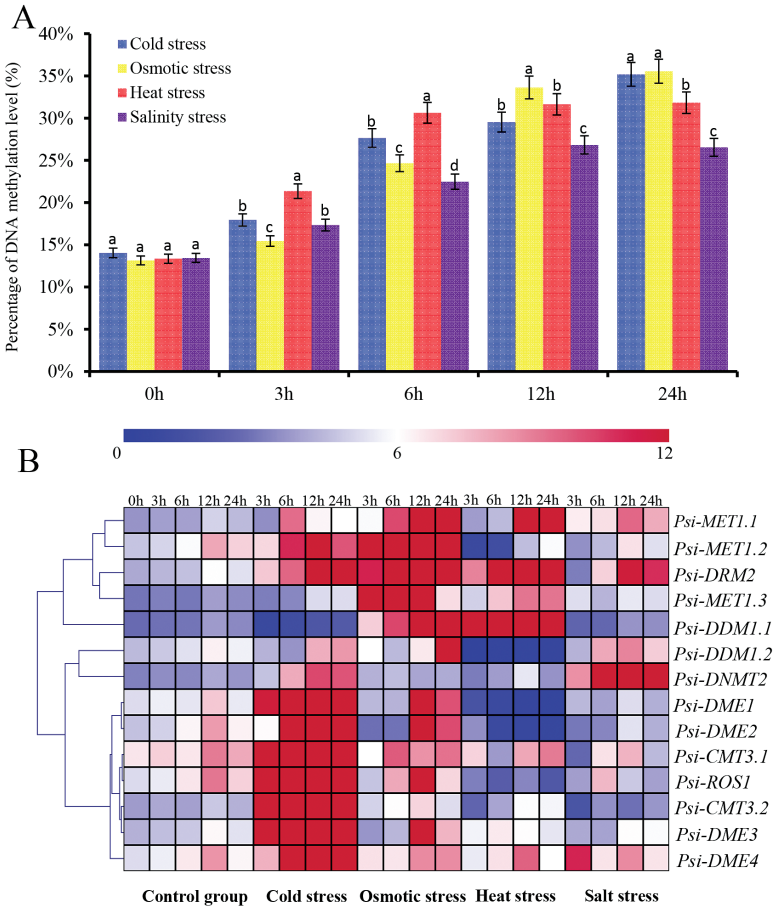

Fig. 1. Genomic DNA methylation levels and DNA methylation-related gene expression under abiotic stress. (A) Dynamic genome DNA methylation level under abiotic stress. Error bars represent the SE. Different letters on error bars indicate significant differences at $P<0.05$. (B) Heatmap of hierarchical clustering for expression of DNA methylation- and demethylation-related genes under abiotic stress. Blue represents lower expression compared with the reference gene, and red denotes higher expression. The colored bar indicates the magnitudes of $\log_2$ expression fold change (fold change >2 or <0.5, $P<0.01$ represent significant differences).

and the cytosine methylation levels under heat stress peaked at 6 h and then remained unchanged until 24 h. In contrast, the cytosine methylation levels under salinity, osmotic, and cold stress treatment gradually increased until 24 h. At 24 h, the cytosine methylation levels under osmotic and cold stress treatment were significantly higher than under heat stress (Fig. 1A).

To examine the gene expression responses underlying this, we also measured the expression of genes encoding methylation-related enzymes. In plants, four classes of DNA methyltransferases participate in the establishment and maintenance of DNA methylation, and two classes of DNA glycosylases participate in demethylation. Here, we profiled the expression of 14 DNA methyltransferase- and glycosylase-related genes under the four abiotic stresses (Fig. 1B; Supplementary Table S4). Under salinity stress, only *PsiDNA METHYLTRANSFERASE 2* (*PsiDNMT2*) was significantly induced; expression of the other genes did not change. Under osmotic stress, transcript levels for methylation-related genes increased, including *PsiDOMAINS REARRANGED METHYLTRANSFERASE 2* (*PsiDRM2*), *PsiMETHYLTRANSFERASE 1* (*PsiMET1*), and *PsiDECREASE IN DNA METHYLATION* (*PsiDDM1*), but expression of demethylation-related genes did not change. Under heat stress, six genes related to establishment and maintenance of DNA methylation responded; transcript levels of *PsiDDM1.1*, *PsiDRM2*, *PsiMET1.3*, and *PsiMET1.1* increased at various times, but expression of *PsiDDM1.2* and *PsiMET1.2* decreased under heat stress. Demethylation-related genes including *PsiREPRESSOR OF SILENCING 1* (*PsiROS1*) and *PsiDEMETER* (*PsiDME*) were also repressed under heat stress. Under cold stress, genes related to establishment and maintenance of DNA methylation were induced, including *PsiCMT3.1*, *PsiCMT3.2*, *PsiDRM2*, *PsiMET1.1*, *PsiDNMT2*, *PsiROS1*, *PsiDME1*, and *PsiDME3*. Thus, different stresses produced different patterns of gene activation (Fig. 1B).

Differences in relative levels and patterns of cytosine methylation under four abiotic stresses

To examine the genome-wide patterns of DNA methylation in response to these stress treatments, we next performed MSAP analysis. A total of 360 primer combinations from 18 *Hpa*II/*Msp*I and 20 *Eco*RI primers (Supplementary Table S5) were used to detect sites of cytosine methylation at the

5′-CCGG-3′ sequence in genomic DNA from *P. simonii* under different stress treatments. Separation of PCR products showed that 39 121 MSAP fragments were differentially amplified from the two digests and revealed polymorphisms in the banding patterns under different stress treatments. According to the methylation state (unmethylated versus methylated at CG or hemimethylated at CHG), we scored the MSAP bands to estimate the relative total methylation level. Relative methylation levels were in the range of 20.52–29.79% and included 9.60–15.17% ^{m}CG and 11.92–14.62% ^{m}CHG. All three relative methylation levels, namely ^{m}CG, ^{m}CHG, and total (^{m}CG+^{m}CHG), were highest under osmotic stress and lowest in the control group (Supplementary Table S6).

To detect the cytosine methylation patterns under different abiotic stresses, we compared differences and similarities in all possible pairwise comparisons of the four abiotic stresses. For stress-specific methylated sites, 2353 fragments (1202 ^{m}CG and 1151 ^{m}CHG) were significantly higher in heat stress than in other abiotic stresses (Fig. 2A). In contrast, 1186 osmotic stress-specific methylated fragments (632 ^{m}CG and 554 ^{m}CHG) were significantly lower than in other abiotic stresses. For common methylated sites among abiotic stress treatments and the control group, 200 (0.5% of all MSAP fragments) methylated fragments (94 ^{m}CG and 106 ^{m}CHG) were conserved among heat, salt, cold, osmotic stress, and the control group (Fig. 2A). Heat and osmotic stress had the most overlapping methylated sites (29.1% of all heat and osmotic stress methylated sites) including 1637 ^{m}CG and 1247 ^{m}CHG (Fig. 2A). In contrast, cold stress had 1183 ^{m}CG sites (17.3% of all cold and heat stress ^{m}CG sites and 18.1% of all cold and salt stress ^{m}CG sites) that overlapped with heat and salt stress, respectively, significantly lower than the other pairwise comparisons. For ^{m}CHG, salt stress and the control group only had 970 overlapping methylated sites (15.8% of salt stress and control group ^{m}CHG sites) (Fig. 2A).

Hierarchical clustering was used to group methylated sites with similar methylation patterns (Fig. 2B). All methylated sites were grouped into 243 possible combinations in response to abiotic stress (Fig. 2C). Methylated patterns enriched in clusters differed significantly under abiotic stresses over the time course. Among these combinations, five main methylation patterns were significantly enriched, accounting for >38.9% of all methylated sites (Fig. 2C). In Cluster 239, 15.5% of sites were rapidly methylated under abiotic stress at 3 h (Fig. 2C). In contrast, in Cluster 165, 9.4% of sites were methylated under abiotic stress until 24 h (Fig. 2C). Clusters 81 and 162 showed that demethylation also occurred throughout the whole response to abiotic stress. Cluster 163 revealed that 10.2% of methylated sites were conserved that did not respond to abiotic stress.

Isolation, characterization, and validation of SDMRs

Based on the polymorphisms of MSAP banding patterns under abiotic stress, we isolated and sequenced a subset of the stress-specific differentially methylated regions (SDMRs).

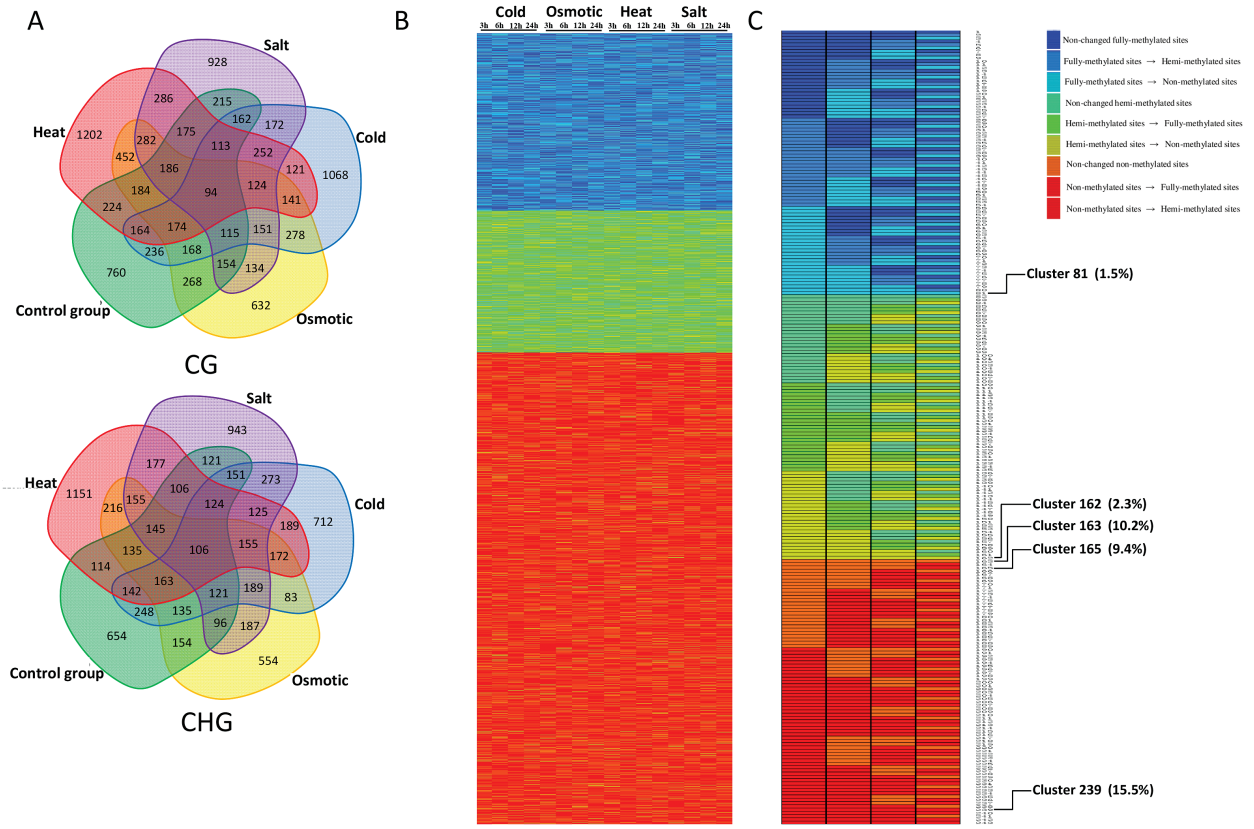

Fig. 2. Global genome DNA methylation pattern in response to abiotic stress. (A) Venn diagram showing the number of methylated sites in response to different abiotic stresses. (B) Heatmap of hierarchical clustering for DNA methylation pattern in response to different abiotic stresses. (C) Diagram showing 243 possible combinations of DNA methylation in response to abiotic stress.

We focused on two groups: Group I includes SDMRs methylated in only one of the four abiotic stresses and the control group. Group II includes SDMRs commonly methylated in all four abiotic stresses. We isolated and identified 400 stress-specific MSAP bands for each abiotic stress and control group, and 200 common MSAP bands for abiotic stress and the control group (~2200 bands). Filtering the failed sequencing and redundant bands, we finally obtained 1376 SDMRs. Annotation analysis of those SDMRs indicated that they are functionally diverse (Supplementary Fig. S2). As indicated in Supplementary Table S7, ~81.6% (1123 sequence) aligned to the *P. trichocarpa* reference genome. Among these genes, 104 protein-coding genes annotated as transcription factors from 29 gene families, 23 protein modification genes, and 68 protein degradation genes (Supplementary Figs S2, S3). For regulation, 39 receptor kinases from eight gene families, 18 involved in calcium regulation, eight G-protein genes, and three mitogen-activated protein (MAP) kinase genes, were found. Sixty-three methylated genes came from large enzyme gene families, including cytochrome P450, glucosidases, peroxidases, UDP glycosyltransferases, GDSL lipases, and β-1,3-glucan hydrolases.

All MSAP fragments were mapped to gene models of the *P. trichocarpa* v3 genome in the promoter (upstream 2 kb), exon, intron, and/or in the 5′- and 3′-flanking regions. Approximately 28% of methylated fragments mapped to gene body regions, with exons and introns accounting for 15.4% and 12.6% of the sites, respectively (Fig. 3A). A total of 21.3% of methylated fragments mapped to promoter regions, more than in the 5′- and 3′-flanking regions (16.9% and 17.8%, respectively). Stress-specific methylated fragments showed different distributions in the four abiotic stresses (Fig. 3A). Most of the heat stress-specific methylated fragments mapped to promoter regions and fewer mapped to intergenic regions, accounting for 23.5% and 14.9% of methylated fragments, respectively. Under cold stress and osmotic stress, only 13.1% and 12.5%, respectively, of methylated fragments mapped to exons and introns, significantly lower than the average value (Fig. 3A).

The other MSAP fragments without protein homology were annotated for conserved miRNAs from miRbase and for novel miRNAs and lncRNAs from transcriptome data in this study (Supplementary Methods S1). In total, 35 methylated fragments were mapped to the precursor sequences of miRNAs and lncRNAs, including five conserved miRNAs, 11 novel miRNAs, and 17 lncRNAs genes. Our mapping results showed that two conserved miRNA genes (*PsiMIR396e* and *PsiMIR166a*) and four novel miRNA genes (*PsiMIR1*, *PsiMIR13*, *PsiMIR21*, and *PsiMIR27*) overlap with loci that encode lncRNAs (Fig. 3B, C). *PsiMIR396e*, *PsiMIR166a*, *PsiMIR1*, *PsiMIR13*, *PsiMIR21*, and *PsiMIR27* genes are located on the antisense strands of *PsiLNCRNA00020674*, *PsiLNCRNA00177789*, *PsiLNCRNA00167707*, *PsiLNCRNA00124808*, and *PsiLNCRNA00201294* (Fig. 3B, C).

We next used methylation-specific PCR (MS-PCR) to validate the results of the MSAP analysis. To that end, 70 MSAP fragment sequences representing 15 stress-specific MSAP bands each from the abiotic stress and control groups, and 15

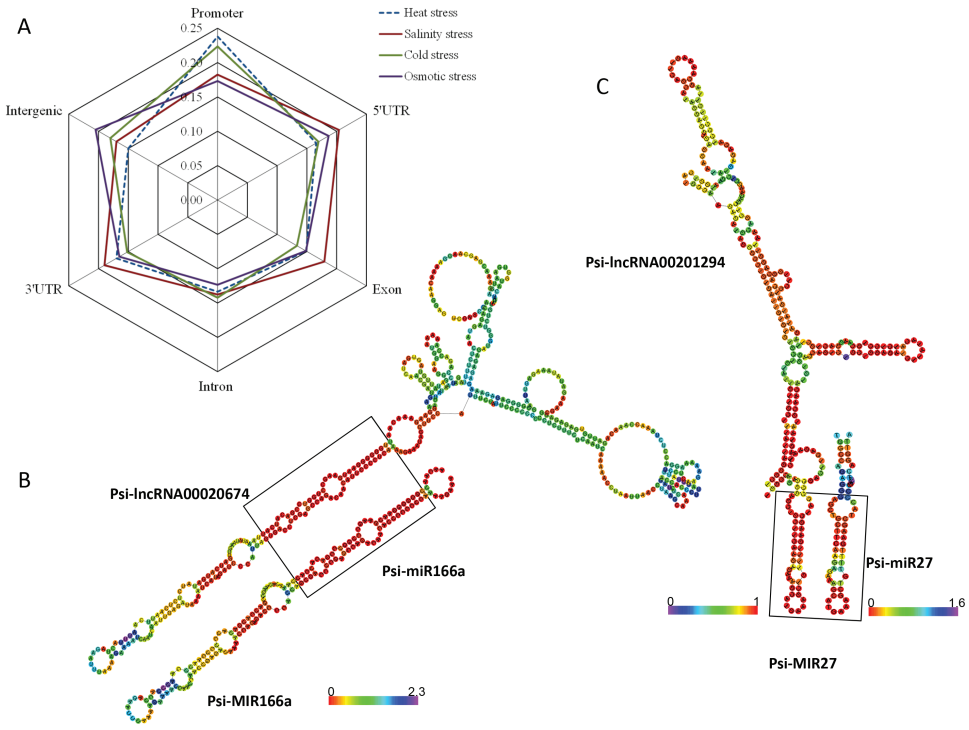

Fig. 3. Distribution and location of stress-specific differentially methylated regions. (A) Distribution of stress-specific differentially methylated regions in the poplar genome. (B and C) Location of stress-specific differentially methylated miRNAs in lncRNA. The black box shows the miRNA sequence. The structure is colored based on base pairing probabilities.

common MSAP bands from abiotic stress and control groups were used to design MS-PCR primers. Filtering the 16 failed sequencing bands (~22.8%), we finally verified 54 methylated sites using MS-PCR (Supplementary Fig. S4), suggesting that MSAP is an effective, stable, and reproducible technology to detect abiotic stress-responsive methylated sites in the poplar genome.

Stress-responsive interactions among DNA methylation, miRNA, and lncRNA genes

Annotation analysis revealed that SDMR162 overlapped with a short, protein-coding gene (*Potri.018G127000*) at base pairs 14 915 179–14 916 946 on chromosome 18. In addition, SDMR162 also overlapped with the *MIR396e* gene and an lncRNA gene (*PsiLNCRNA00268512*) (Table 1; Supplementary Table S8). *PsiMIR396e* is located in the first exon of *Potri.018G127000*, which contains three exons and two introns. *PsiLNCRNA00268512* has four exons and three introns; the methylated sites detected by MSAP occur in the first exon (Fig. 4A). Also, *PsiLNCRNA00268512* is located on the antisense strand of *Potri.018G127000* and has substantial overlap. *PsiMIR396e* is located in the first exon of *Potri.018G127000*, which has three exons and two introns. *PsiLNCRNA00268512* has four exons and three introns that included methylated sites detected by MSAP located in the first exon. The second exon is in the complementary strand of the third exon of *Potri.018G127000*. The third exon is in the complementary strand of the second exon of *Potri.018G127000*, except four nucleotides that contain a splicing site. The fourth exon is in the complementary strand of the first exon of *Potri.018G127000* and extends 250 bp past the transcription start site (Fig. 4A). Based on the sequences of *PsiLNCRNA00268512* and *PsiMIR396e*, we predicted that PsilncRNA00268512 interacts with miR396e-3p and miR396e-5p. The interaction energies indicated that the lncRNA interaction with miR396e-3p (–39.92 K cal^{-1}) was more stable than with miR396e-5p (–36.04 K cal^{-1}) (Fig. 4A; Supplementary Fig S5).

We selected *SDMR162* to perform bisulfite genomic sequencing for each of the four abiotic stresses over a time course. The methylation levels of CG, CHG, and CHH on the sense strand were substantially higher (31.83–34.21%) than on the antisense strand under cold and osmotic stress (Fig. 4B). In contrast, under heat and salt stress, the methylation levels of CG, CHG, and CHH on the antisense strand were substantially higher (35.25–39.65%) than on the sense strand. In the time course, the methylation level of sense and

Table 1. *Location of microRNAs, lncRNAs, and host genes*

Type	No.	Genome location	Methylated regions	Methylation patterns	Target genes[a]	Description[b]
miRNA	miR396e-3p	Chr18:14914436–14914456	Promoter	Methylation	Potri.001G124300	Putative aspartate–arginine-rich mRNA binding protein mRNA
					Potri.018G081000	AAA-type ATPase family protein
					Potri.009G130600	Zinc finger (CCCH-type) family protein
	miR396e-5p	Chr18:14914544–14914565	Promoter	Methylation	Potri.001G215800	Similar to DNAJ heat shock N-terminal domain-containing protein
					Potri.006G066800	WD-40 repeat family protein
					Potri.007G090400	Similar to acyl CoA oxidase homolog
					Potri.014G007200	Similar to transcription activator GRL1
lncRNA	TCONS_00268512	Chr18:14913689–14917000	Promoter	Methylation	miR396e-3p miR396e-5p	
Hostgene	Potri.018G127000	Chr18:14915179–14916946	Promoter	Methylation		
miRNA	miR166a	Chr01:6620351–6620372	Promoter	Methylation		
lncRNA	TCONS_00020674	Chr01:6620264–6622910	Promoter	Methylation		
miRNA	Psi-miR1	Chr10:3868082–3868103	Gene body	Methylation	Potri.001G071100	Similar to 60S ribosomal protein L21
lncRNA	TCONS_00177789	Chr10:3867315–3874863	Gene body	Methylation		
miRNA	Psi-miR13	Chr06:21595863–21595884	Promoter	Methylation	Potri.001G241700	SCARECROW-like 14
lncRNA	TCONS_00124808	Chr06:21595584–21596205	Promoter	Methylation		
miRNA	Psi-miR27	Chr12:11659317–11659338	Promoter	Methylation	Potri.008G023100	Ferric reductase transmembrane component family
lncRNA	TCONS_00201294	Chr12:11659062–11659798	Promoter	Methylation		

[a] Target genes were obtained from psRNATarget tools (http://plantgrn.noble.org/psRNATarget)
[b] Annotation were obtained from the JGI (http://phytozome.jgi.doe.gov/pz/portal.html).

antisense strands increased gradually, and *de novo* methylation and demethylation occurred simultaneously. The methylation level increased faster under heat stress than under other abiotic stresses (Fig. 4B).

Expression of *MIR396e-5p* and *MIR396e-3p* differed significantly; *MIR396e-5p* transcript abundance was >100-fold higher than that of *MIR396e-3p* under four abiotic stresses and in the control group (Fig. 4A). Compared with the control group, *MIR396e-3p* was significantly up-regulated by 35.1-, 2.3-, 5.3-, and 20.6-fold under salt, osmotic, cold, and heat stress, respectively. In contrast, *MIR396e-5p* was significantly up-regulated by 3.2-, 6.5-, and 11.8-fold under osmotic, cold, and heat stress, respectively (Fig. 4A). In the time course, *MIR396e-3p* expression was induced at 3 h, peaked at 6 h, and then decreased gradually. In contrast, *MIR396e-5p* expression was stable from 3 h to 24 h. *PsiLNCRNA00268512* was significantly up-regulated by 26.9- and 2.1-fold under osmotic and cold stress, respectively (Fig. 4A). In the time course, *PsiLNCRNA00268512* transcript abundance decreased from 12 h. *Potri.018G127000* expression was significantly up-regulated under salt and cold stress from 3 h to 24 h. At 6 h, *Potri.018G127000* expression increased to a peak under osmotic and heat stress and then decreased gradually (Fig. 4A).

Correlation of DNA methylation changes and gene expression

To detect the relationship between changes in DNA methylation and gene expression, all non-coding RNA genes (16 miRNA genes and 17 lncRNA genes) and 20 SDMRs with methylation changes in different regions of genes, including the promoter, intron, exon, and UTRs, were selected for bisulfite sequencing and gene expression analysis. In protein-coding genes, the average cytosine methylation level was highest in exons and lowest in UTRs. During the treatment time course, the average cytosine methylation level of promoters increased significantly to a peak (27%) at 6 h, and then slightly decreased until 24 h. The average cytosine methylation level of introns and exons showed the same tendencies

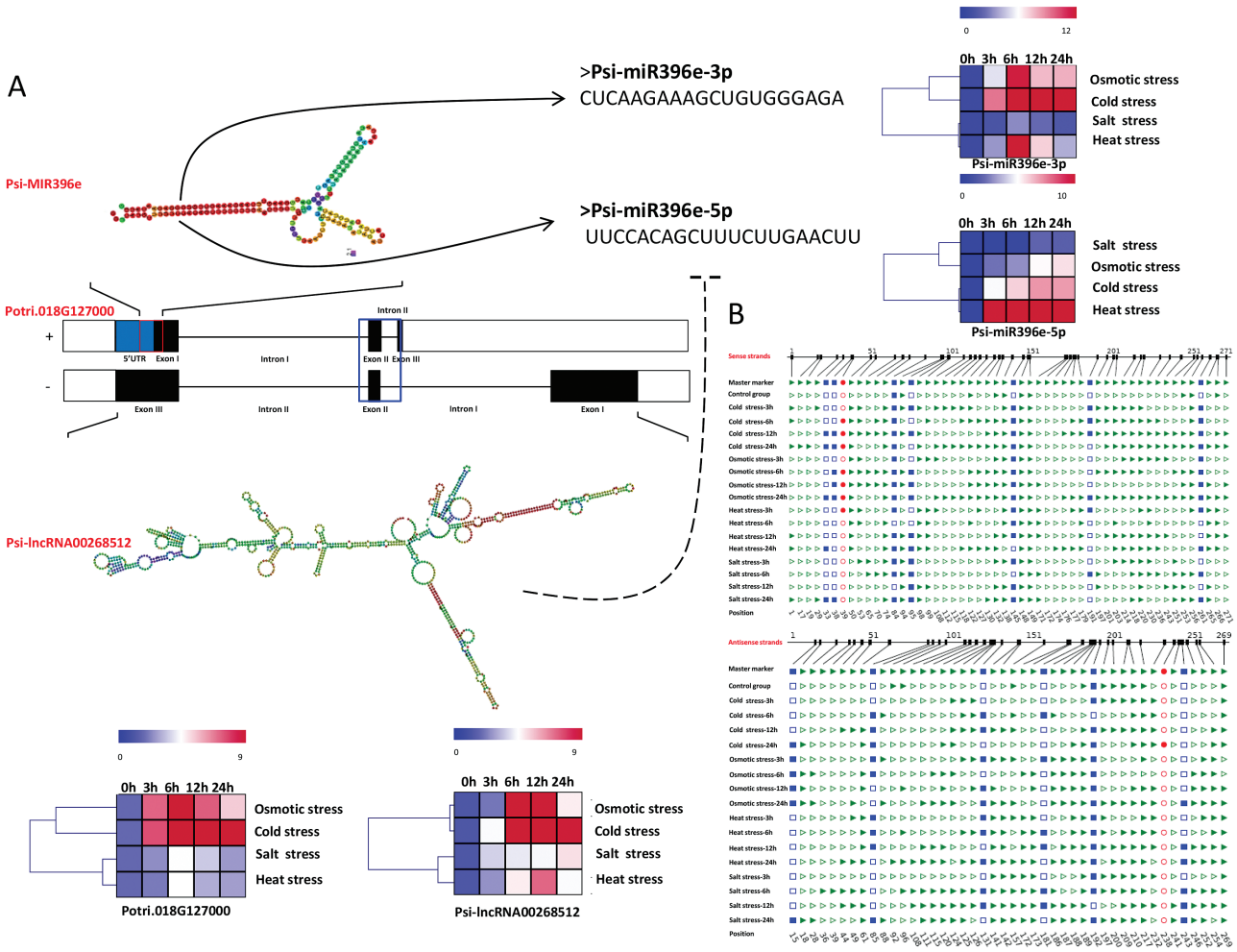

Fig. 4. Diagram of the relationship of the protein-coding genes, lncRNAs, and miRNAs. (A) Location of Potri.18G127000, *MIR396e*, and PsilncRNA00268512 in the genome. '+' represents sense strands; '–' represents antisense strands. Heatmaps represent the expression patterns of protein-coding gene, miRNA, and lncRNA. Blue represents lower expression compared with the reference gene, and red denotes higher expression, with values indicating the magnitude of $\log_2$ expression fold change. (B) Abiotic stress-responsive DNA methylation patterns of candidate regions located in the blue box of the protein-coding gene. Filled red circles denote ^{m}CG; open red circles denote CG; filled blue squares denote ^{m}CHG; open blue squares denote CHG; filled green arrowheads denote ^{m}CHH; and open green arrowheads denote CHH.

as promoter regions, but with lower methylation levels. The average cytosine methylation level of UTRs increased to a peak (22%) at 12 h. In contrast, in non-coding RNA genes, the average methylation levels of promoters were higher than those of transcribed regions from 0 h to 24 h. Methylation levels of promoters and transcribed regions increased to a peak (25% and 23%) at 6 h and 12 h, respectively.

Correlation analysis of gene expression and methylation changes in different regions showed that expression of protein-coding genes showed a significant negative correlation with methylation changes in promoters, introns, exons, and UTRs ($r_{mC\text{-}Promoter}$= −0.81, P<0.01; $r_{mC\text{-}intron}$= −0.78, P<0.01; $r_{mC\text{-}exon}$= −0.74, P<0.01; $r_{mC\text{-}UTRs}$= −0.63, P<0.01), respectively (Fig. 5A). Expression of non-coding genes also showed a significant negative correlation with methylation changes in promoters and transcribed regions ($r_{mC\text{-}Promoter}$= −0.82, P<0.01; $r_{mC\text{-}transcribed\ regions}$= −0.65, P<0.01), respectively (Fig. 5B).

Expression of methylated miRNAs and their targets in response to abiotic stress

The loci encoding five conserved miRNA genes (*MIRNA167-3p*, *MIR6445a*, *MIRNA319c*, *MIR156f*, and *MIR472a*) and 11 novel miRNAs were methylated under abiotic stress (Table 2). Quantitative PCR analysis showed that cleaved transcripts of targets were positively correlated with miRNA gene expression (Supplementary Fig. S6). The miR6445a targets *DEHYDRATION-RESPONSIVE ELEMENT-BINDING PROTEIN 1D* (*DREB1D*), *HEAT SHOCK PROTEIN 70* (*HSP70*), *HIGHLY ABA-INDUCED PP2C GENE 3* (*HAI3*), and the *MIR6445a* gene were methylated at 3 h under salt stress and at 12 h under osmotic, cold, and heat stress. Their expression was induced from 3 h to 6 h under osmotic, cold, and heat stress, and then was repressed at 12 h. Under salt stress, expression of all three targets significantly and steadily increased, compared with expression in control, untreated plants. In contrast, expression of all three targets significantly increased until 12 h under osmotic and cold stress. Under heat stress, expression of *Psi-DREB9* and *Psi-HSP70* was induced starting at 3 h stress treatment; in contrast, *Psi-HAI3* expression was induced until 12 h of stress treatment (Fig. 6). Thus, the different targets of miR6445a showed different patterns of stress-responsive expression.

PsiMIR156f was methylated in the control group, and its methylation did not change under osmotic and cold stress. The expression of *MIR156f* did not change under osmotic stress, but decreased significantly under cold stress from 3 h to 24 h. In contrast, PsiMIR156f was demethylated at 3 h under heat and salt stress and miR156f transcript abundance significantly increased from 3 h to 24 h under heat and salt stress. Expression of *SQUAMOSA PROMOTER BINDING PROTEIN* (*SBP*)*-DOMAIN TRANSCRIPTION FACTOR 6* (*SPL6*), a target of miR156f, did not respond to osmotic and cold stress and significantly decreased under heat and salt stress from 3 h to 24 h (Fig. 6).

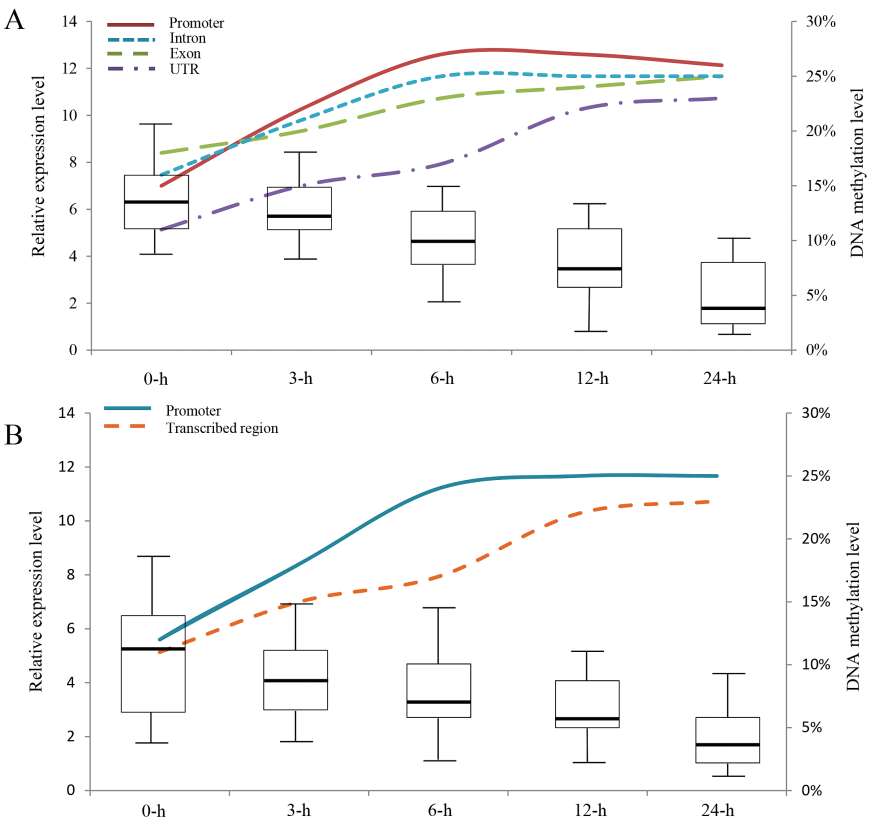

Fig. 5. Association of protein-coding gene and non-coding gene expression with methylation. (A) Box plots representing the association of protein-coding gene expression with DNA methylation in different regions. (B) Box plots representing the association of miRNA gene expression with DNA methylation in different regions. 0-h represents control group gene expression, 3-h to 24-h represent the time course of abiotic stress treatment.

Table 2. *Methylated miRNA genes and their targets*

No.	Sequence/genome location	Methylated regions	Methylation patterns	Target genes[a]	Cleavage site	Description[b]
Ptc-miR6445a	TTCATTCCTCTTCCTAAAATGG/ Chr12:7706152–7706293	Promoter	Methylation	Potri.001G110700	298	Similar to dehydration responsive element binding protein 1 like protein(DREB9)
				Potri.008G054800	604	Similar to heat shock protein 70 cognate
				Potri.T137100	763	Highly ABA-induced PP2C gene 3 (HAI3)
				Potri.002G153800	43	Peroxisomal biogenesis factor 11 family protein
Ptc-miR156f	TGACAGAAGAGAGTGAGCAC/ Chr18:12448484–12448584	Gene body	Demethylation	Potri.002G052800	477	Similar to cyclin 2
				Potri.010G154300	1180	Similar to squamosa promoter-binding protein-like 6 (SPL6)
Ptc-miR472a	TTTTCCCTACTCCACCCATCCC/ Chr5:119630–119710	Promoter	Demethylation	Potri.003G101000	138	NB-ARC domain-containing disease resistance protein
				Potri.005G042900	738	Similar to putative disease resistance gene analog NBS-LRR
Psi-miR5	GTTCCATTTCTGATTCTAGGC/ Chr10:14521310–14521330	Promoter	Methylation	Potri.014G028200	1051	Similar to bZIP transcription factor 6. (Pt-ABF2.1)
				Potri.002G125400	1082	Similar to bZIP transcription factor 6. (Pt-ABF2.2)
Psi-miR14	AAGGCATGGGAGATACTGAAA/ Chr12:295244–295264	Promoter	Methylation	Potri.014G028200	1213	Similar to bZIP transcription factor 6. (Pt-ABF2.1)
				Potri.002G125400	1246	Similar to bZIP transcription factor 6. (Pt-ABF2.2)
Psi-miR67	CTTAGAAGTAGAGACAGGATT/ Chr2:16497643–16497663	Gene body	Demethylation	Potri.001G222600	323	Similar to CBL-INTERACTING PROTEIN KINASE 3
				Potri.002G256600	552	Similar to auxin-responsive protein
				Potri.005G073900	704	DNAJ heat shock family protein

[a] Target genes were obtained from psRNATarget tools (http://plantgrn.noble.org/psRNATarget).
[b] Annotation were obtained from the JGI (http://phytozome.jgi.doe.gov/pz/portal.html).

PsiMIR472b was demethylated at 3 h under cold, heat, and salt stress, and until 12 h under osmotic stress. Under osmotic stress, miR472b levels significantly increased until 12 h. In contrast, miR472b rapidly increased at 3 h under cold, heat, and salt stress. Expression of two targets of miR472b, *Potri.005G042900* and *Potri.003G101000* (a defense gene encoding an NB-ARC domain-containing disease resistance protein), did not respond to osmotic and cold stress and significantly decreased under heat and salt stress from 3 h to 24 h (Fig. 6).

PsiMIR5 and *PsiMIR14*, two target homologs of *ABSCISIC ACID RESPONSIVE ELEMENTS-BINDING FACTOR 2* (*ABF2*), were methylated at 6 h under osmotic and cold stress and at 12 h under heat and salt stress. The expression of *PsiMIR5* and *PsiMIR14* was repressed from 6 h under osmotic and cold stress and from 12 h under heat and salt stress. *ABF2.1* expression did not respond to osmotic stress and salt stress but sensitively responded to cold and heat stress. In contrast, *ABF2.2* expression just responded to salt stress. *PsimiR67* was demethylated at 3 h in response to all four abiotic stresses. Expression of *CBL-INTERACTING PROTEIN KINASE 3* (*CIPK*), a target of PsimiR13, was significantly induced at 3 h under the four abiotic stresses (Fig. 6).

Stability of stress-responsive methylation sites

We measured the stability of methylation at all sites during long-term growth in the greenhouse at 1, 2, and 6 month time points. For the control group, 87.9% of methylation sites were not changed after 1 and 2 months. After 6 months, ~64.8% of methylation sites were preserved. In contrast, only 8414 of 22 832 *de novo* methylation sites (~35.1%) were detected at 1 month after abiotic stress, including 6192 ^{m}CG sites and 2222 ^{m}CHG sites. After 2 months, only 23.8% of *de novo* methylated sites were detected. After 6 months, when new leaves had grown after dormancy, only 15.3% of *de novo* methylation sites were detected (2165 ^{m}CG sites and 1328 ^{m}CHG sites). For 16 289 demethylation sites that responded to short-term abiotic stress, 28.9, 17.7, and 11.3% of sites were detected after 1, 2, and 6 months, respectively. Following cold stress, 18.7% of *de novo* methylated sites were detected after 6 months and, following osmotic stress, 17.6% of sites were detected, significantly more than for heat and salt stress (Supplementary Table S9).

Among 1376 SDMRs, 373, 289, and 164 SDMRs were detected 1, 2, and 6 months after the abiotic stress. Functional enrichment analysis of genes in these SDMRs showed that genes involved in regulation of nitrogen compound metabolic process, macromolecule biosynthetic process, and

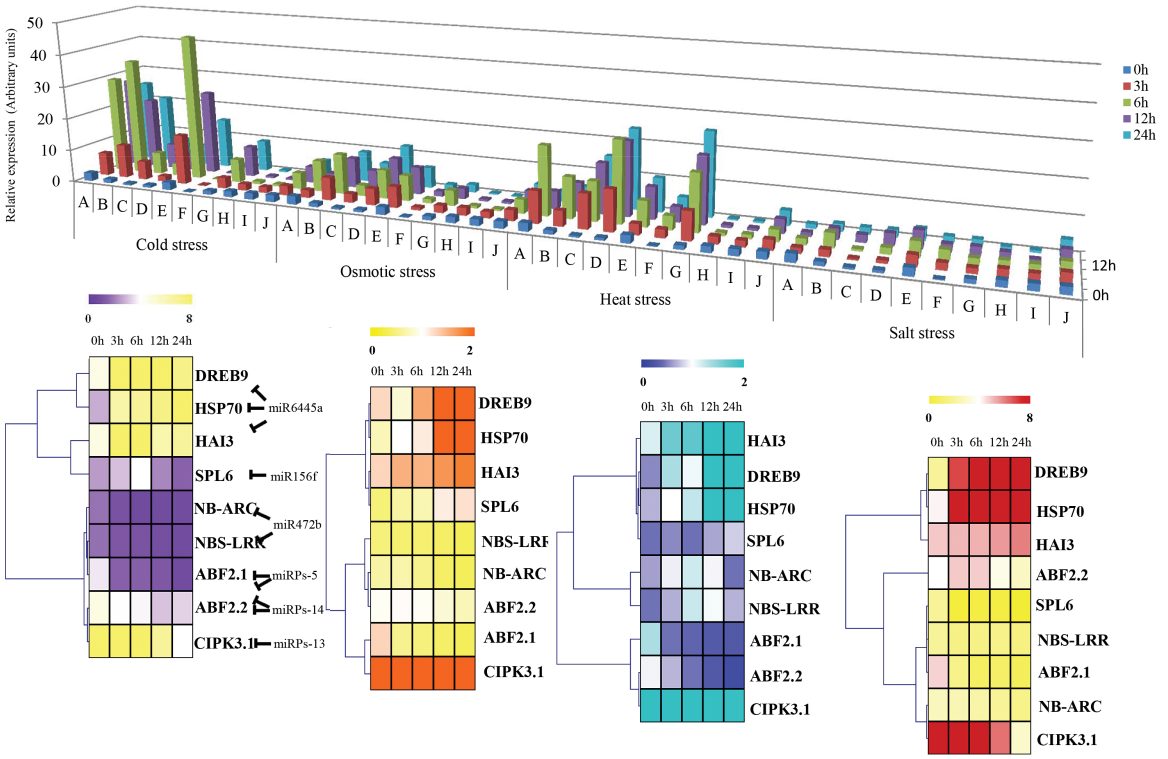

Fig. 6. Expression of methylated miRNA genes and their targets under abiotic stress. The histogram shows methylated miRNA gene expression in response to abiotic stresses. The heatmap shows expression of their targets under abiotic stress. Values of color scale bars indicate the magnitude of $\log_2$ expression fold change. A, miR6445a; B, miR396e-3p; C, miR396e-5p; D, miR167g-3p; E, miR319c; F, miR156f; G, miR472a; H, PsimiR5; I, PsimiR67; J, PsimiR14.

photosynthesis were enriched. A total of 164 SDMRs maintained their methylated status at 6 months, including genes encoding four transcription factors (ZIP, bHLH, MADS, and TCP families), eight signaling receptor kinases, and five protein modification factors (Supplementary Table S10). The 76 and 59 SDMRs methylated at 6 months after cold and osmotic stress represent genes for biological processes enriched in cell wall modification and carbohydrate biosynthetic process. Only 27 and 39 SDMRs were methylated 6 months after heat and salt stress, and they represent genes with no significant enrichment for biological process and molecular function. Among these SDMRs, eight were steadily co-methylated under four abiotic stresses, namely SDMR9, 61, 144, 213, 268, 413, 652, and 1260, which represent *METHYLCROTONOYL-COA CARBOXYLASE* (*Pt-MCCA.1*), *GLYCERALDEHYDE-3-PHOSPHATE DEHYDROGENASE* (*Pt-GAPDH1.1*), *PHOTOSYSTEM I REACTION CENTER SUBUNIT PSAK* (*Pt-PSAK.2*), *WRKY TRANSCRIPTION FACTOR 6* (*Pt-WRKY6.1*), *AUXIN EFFLUX CARRIER PROTEIN 10* (*Pt-PIN2.3*), *CHLOROPHYLL A-B BINDING PROTEIN 2* (*Pt-LHB1.3*), ethylene-inducible ER33 protein, *EARLY LEAF SENESCENCE ABUNDANT CYSTEINE PROTEASE* (*Pt-ELSA.1*), and zeaxanthin epoxidase (*Pt-ABA1*), respectively. Of the methylated miRNA genes, only *PsiMIR6445a* maintained its methylated status after 6 months (Fig. 7). In contrast, *PsiMIR472b* was re-methylated 1 month later. At 1 month later, MIR6445a expression in different abiotic stress treatment groups did not differ significantly from that in the control group. Expression of all three target genes was still significantly higher in the abiotic stress groups than in the control group. Because the DNA methylation level was lower in the heat and salt stress treatment groups (Supplementary Fig. S7), expression of methylated *PsiMIR472b* in the heat and salt stress treatment group was repressed but still significantly higher than in the osmotic and cold stress groups. Expression of two targets of miR472a, including the NB-ARC domain-containing disease resistance-related gene, was still lower in the heat and salt stress treatment groups than in the osmotic and cold stress treatment groups.

Discussion

Differences in relative levels and patterns of cytosine methylation in response to different abiotic stresses

Recent work has demonstrated the common link between abiotic stress and DNA methylation, and indicated that the response patterns might be species specific (Boyko and Kovalchuk, 2007; Boyko *et al.*, 2010). In this study, we have shown that cytosine methylation levels increased significantly after 3 h of treatment in response to four different abiotic stresses, suggesting that abiotic stress also rapidly triggers DNA methylation in poplar. Our study also showed that the cytosine methylation level under heat stress was significantly higher than that under osmotic, cold, or salinity stress at 3 h and 6 h, and osmotic and cold stress induced significantly

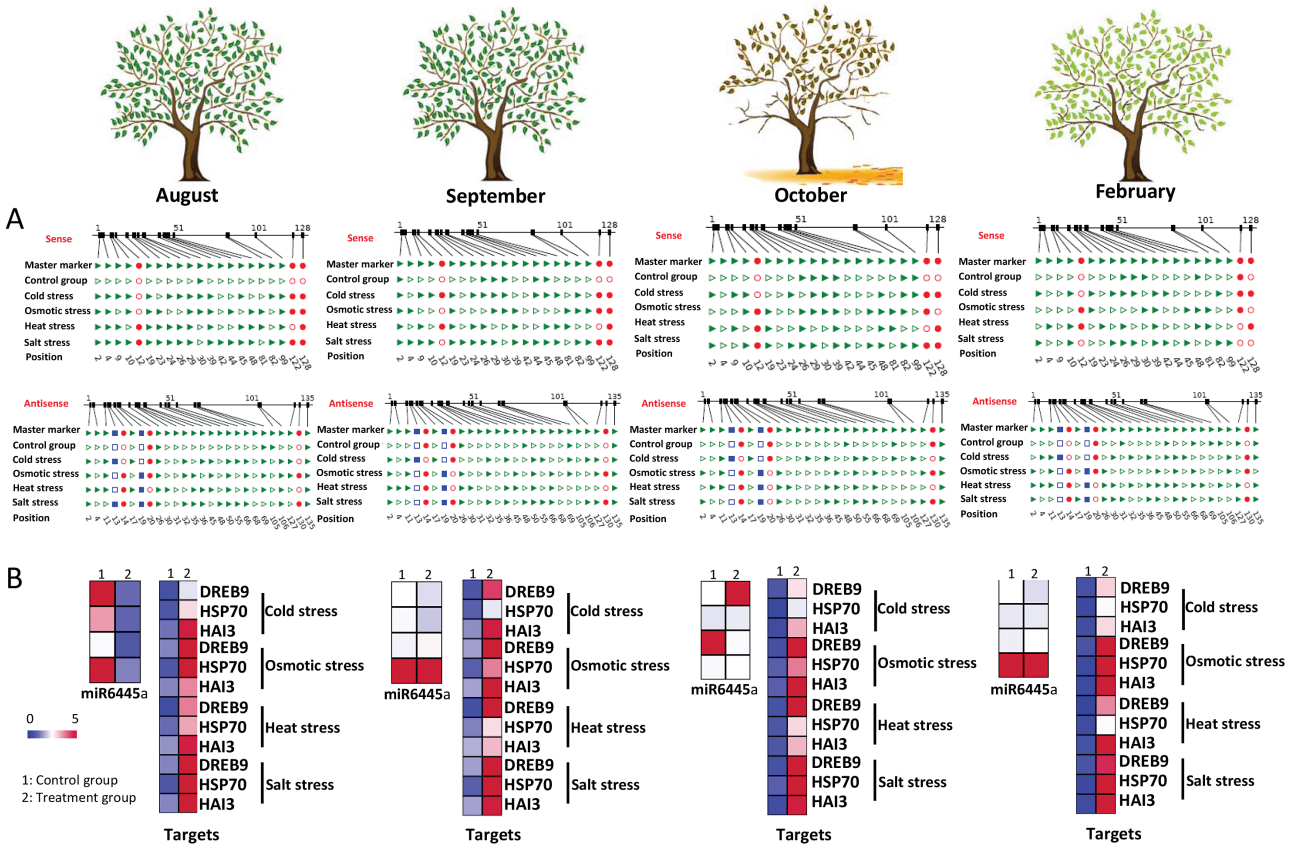

Fig. 7. Stability of DNA methylation of the *Psi-MIR6445a* gene after abiotic stress and long-term expression patterns of miRNA6445a and its targets. (A) Dynamic sense and antisense DNA methylation pattern of *Psi-MIR6445a* after abiotic stress. Filled red circles denote ^{m}CG; open red circles denote CG; filled blue squares denote ^{m}CHG; open blue squares denote CHG; filled green arrowheads denote ^{m}CHH; and open green arrowheads denote CHH. (B) Heatmap showing the expression of the methylated *Psi-MIR6445a* gene and the targets of miR6445a. 1, the control group; 2, the treatment group. Blue represents lower expression compared with the reference gene, while red denotes higher expression. The color bar indicates the magnitudes of $\log_2$ expression fold change (fold change>2 or <0.5, P<0.01represent significantly different).

higher cytosine methylation levels than heat and salinity stress at 24 h, suggesting that DNA methylation levels and patterns differ among the four abiotic stresses. Thus, we conclude that DNA methylation might be a rapid and sensitive epigenetic regulation mechanism acting in response to multiple abiotic stresses in poplar.

Experimental evidence suggests the existence of four distinct classes of enzymes responsible for cytosine methylation establishment and maintenance, namely DRM2, MET1, DNMT2, and CMT3 (Chan *et al.*, 2005). DRM2 methyltransferase functions in establishment of *de novo* DNA methylation (Cao *et al.*, 2000). MET1 and CMT3 methyltransferases function in maintenance of CG and non-CG methylation, respectively (Malagnac *et al.*, 2002; Saze *et al.*, 2003). The DNMT2 class of methyltransferase is conserved in many eukaryotic genomes but its function is unknown (Chan *et al.*, 2005). DDM1 has ATPase activity and can remodel nucleosomes (Brzeski and Jerzmanowski, 2003). Arabidopsis *ddm1* mutants lack both CG methylation and methylation of lysine residue K9 in histone H3 (H3-K9) at heterochromatic loci (Gendrel *et al.*, 2002; Lippman *et al.*, 2004). In this study, *PsiDNMT2* was significantly induced and correlated with increases in DNA methylation level under salinity stress, suggesting that *PsiDNMT2* might function in salinity stress-specific establishment of DNA methylation. Under osmotic stress, *PsiDRM2*, *PsiMET1*, and *PsiDDM1* were significantly induced, suggesting that expression of these genes triggers *de novo* DNA methylation, and maintenance of CG methylation might be the main cause of the increased DNA methylation level. *PsiMET1.2*, *PsiMET1.3*, and *PsiDDM1.2* were significantly induced at 3 h, but *PsiMET1.1* and *PsiDDM1.1* were significantly up-regulated at 6 h and 24 h, respectively, suggesting that different members of the *PsiMET1* and *PsiDDM1* families function in different phases of osmotic stress responses. Compared with the other abiotic stresses, *PsiMET1.2* and *PsiDDM1.2* were induced only under osmotic stress, indicating that they might show stress-specific expression. *PsiDRM2*, *PsiMET1.3*, and *PsiDDM1.1* were significantly induced at different phases of heat stress, suggesting that, compared with osmotic stress, *de novo* DNA methylation and maintenance of CG methylation were also induced in heat stress. Under cold stress, *PsiCMT3.1* and *PsiCMT3.2* expression were significantly up-regulated along with *PsiDRM2*, *PsiMET1.1*, and *PsiDNMT2* expression, suggesting that maintenance of CHG methylation was induced specifically by cold stress.

DNA glycosylases can initiate base excision repair by cleaving the DNA backbone at the base-removal site (Krokan *et al.*, 1997). *ROS1* functions as a demethylase by removing methylated cytosine residues from DNA (Gong *et al.*, 2002).

DME functions antagonistically to *MET1* in the control of seed development (Xiao *et al.*, 2003). Our result showed that the poplar (*P. trichocharpa*) genome has only one copy of *ROS1* and four copies of *DME*. Expression of these genes did not change under salinity and osmotic stress, suggesting that demethylation did not respond to salinity and osmotic stress. *PsiROS1*, *PsiDME1*, and *PsiDME2* expression significantly decreased under heat stress, suggesting that demethylation was repressed. Repressed demethylation correlates with induced *de novo* methylation. This might result in the highest methylation level at the beginning of heat stress. Under cold stress, *PsiROS1*, *PsiDME1*, and *PsiDME3* were significantly induced, suggesting that establishment of methylation and demethylation occurred simultaneously.

Patterns of DNA methylation in the regulation of gene expression

More evidence demonstrates that non-coding RNA molecules play essential roles in the regulation of gene expression (Ponting *et al.*, 2009; Wilusz *et al.*, 2009). For example, miRNAs negatively regulate gene expression at the transcriptional and/or post-transcriptional levels by degrading or inhibiting the translation of target mRNAs (Carthew and Sontheimer, 2009; Voinnet, 2009; Chen, 2010). In contrast, lncRNAs are non-protein-coding RNAs of >200 bp in length, distinct from miRNAs and small interfering RNAs (siRNAs) (Zhu and Wang, 2012). According to their genomic organization, intergenic miRNA genes, intragenic miRNA genes, and lncRNAs can be further grouped into antisense lncRNAs, intronic lncRNAs, overlapping lncRNAs (which partially overlap protein-coding genes), and intergenic lncRNAs (Rinn and Chang, 2012). Our study identified *PsiMIR396e* and *PsiLNCRNA00268512*, located in an exon and on the antisense strand, respectively, of the methylated gene *Potri.018G127000*, indicating that this locus might comprise several complex transcriptional units regulated by DNA methylation in the poplar response to abiotic stresses.

The relationship between DNA methylation and gene expression has been extensively studied. It appears that different species and methylated regions in genes have different effects on gene expression (Flores *et al.*, 2012; Song *et al.*, 2015). Gene methylation in promoter regions is generally associated with the repression of gene expression (Zhang *et al.*, 2006). In contrast, intragenic DNA methylation and gene expression showed a positive linear correlation in anemone and silkworm (Xiang *et al.*, 2010; Zemach *et al.*, 2010). Other organisms, including honeybee, Arabidopsis, and poplar, showed a parabolic relationship, in which most moderately transcribed genes are more methylated than genes with low or high expression (Zhang *et al.*, 2006; Vining *et al.*, 2012). Our results showed the strongest negative correlation of promoter methylation with expression of protein-coding genes and non-coding RNA genes, suggesting that promoter methylation might mainly play a role in gene expression regulation under abiotic stress. Vining *et al.* (2012) indicated that, in poplar, gene length might be closely associated with DNA methylation levels and pattern, and with the regulation of gene expression (Vining *et al.*, 2012). Our results also showed different correlations of gene expression and methylation in exons, introns, transcribed regions, and UTRs, implying that the average length of these DNA elements might be an important reason for this divergence.

A previous study suggested that RNAs might influence each other by competing for miRNA response elements (MREs) (Salmena *et al.*, 2011). This 'competing endogenous RNA' activity forms a large-scale regulatory network across the transcriptome, including protein-coding genes, pseudogenes, miRNA genes, and lncRNA genes. Poliseno *et al.* (2010) found that *PHOSPHATASE AND TENSIN HOMOLOG* (*PTEN*), a tumor suppressor gene, shares many MREs with its pseudogene *PHOSPHATASE AND TENSIN HOMOLOG PSEUDOGENE 1* (*PTENP1*), and overexpression of the *PTENP1* 3′-UTR increased levels of *PTEN* and growth inhibition in a DICER-dependent manner. *PTENP1* could be considered a competitor for miRNA494, which targets *PTEN* (Poliseno *et al.*, 2010). Our results showed that PsilncRNA00268512 interacts with miR396e, and the lncRNA interacts with miR396e-3p, which was more stable than the interaction with miR3-5p, and suggested that the lncRNA competing miR396e-3p might affect its transcript abundance, causing it to be significantly lower than the abundance of miR396e-5p. Under cold and osmotic stress, lncRNA transcript abundance increased associated with a decrease in minus-strand methylation levels, resulting in down-regulation of miRNA396e-3p and -5p. This implies that DNA methylation regulated a cascade reaction of non-coding RNA in poplar genome response to abiotic stress.

DNA methylation affects the abiotic stress response regulatory network of miRNAs

Previous studies have demonstrated that epigenetic modifications also regulate the expression of miRNA genes (Bracken *et al.*, 2008; Vrba *et al.*, 2010). In mammals, methylation in miRNA promoters resulted in repressed expression in many cancer types (Li *et al.*, 2011). In contrast, DNA methylation and miRNA expression may have a complex interaction in plants. The 21 nt RNAs generally repress expression of their target genes through mRNA cleavage, while 24 nt miRNAs can direct cytosine DNA methylation at their own loci *in cis* and at their target genes *in trans*, resulting in transcriptional gene silencing (Wu *et al.*, 2010). Our results showed that five conserved miRNA genes and 11 novel miRNA genes were methylated under abiotic stress, suggesting that abiotic stress-responsive DNA methylation in miRNA genes exists in poplar. Of the 16 methylated miRNA genes, only *PsimiR1* belongs to the long miRNAs (~24 nt), implying that abiotic stress-responsive DNA methylation is biased toward canonical miRNAs (~21 nt).

MiRNAs negatively regulate gene expression by degrading or inhibiting the translation of target mRNAs (Chen, 2010). Our results showed that six of 16 methylated miRNA genes target seven known abiotic and biotic stress-responsive genes. The abiotic stress-responsive group includes *PsiDREB1D*, *PsiHSP70*, *PsiHAI3*, *PsiABF2*, and *PsiCIPK3*, which

participate in transcriptional regulation and signal transduction. The biotic stress-responsive group includes *PsiSPL6* and *PsiNB-ARC*, implying that DNA methylation might regulate the crosstalk of abiotic and biotic stress responses in the plant genome. The loci producing miR6445a, PsimiR5, and PsimiR14 were methylated under abiotic stresses at different time points, suggesting that the methylation of these miRNA genes differs among different abiotic stresses. With the repressed expression of these methylated miRNA genes, expression of their targets was induced to different extents. For example, *DREB1D* acts in abscisic acid (ABA)-activated signaling pathway-mediated regulation of transcription. Overexpression of the *AtDREB1D* transcription factor gene could significantly enhance drought tolerance in plants (Guttikonda *et al.*, 2014). *HSP70* acts in protein folding and ubiquitination, regulation of transcription, and responses to abiotic and biotic stress (Zhou *et al.*, 2014). *HAI3* acts in protein amino acid dephosphorylation in response to ABA signaling (Bhaskara *et al.*, 2012). *ABF2* binding to the ABA-responsive element (ABRE) motif in the promoter region of ABA-inducible genes enhances drought tolerance in plants (Des Marais *et al.*, 2014). DNA methylation repressed the expression of a negative regulator of these targets, thus playing a positive role in enhancing abiotic stress tolerance in plants. Moreover, expression of *PsiDREB9* and *PsiHSP70* was not significantly repressed with high transcript abundance of miR6445a under heat stress, suggesting the possible existence of another regulatory factor for transcriptional regulation of these targets. Expression of *PsiSPL6*, *Potri.005G042900*, and *Potri.003G101000*, genes related to disease resistance, decreased; this was associated with demethylation of the *PsiMIR156f* and *PsiMIR472b* loci, suggesting that abiotic stress might reduce disease resistance of poplar via regulation of DNA methylation.

Long-term effect of DNA methylation in transcription

DNA methylation causes stable alterations in gene activity through diverse mechanisms, including miRNAs and lncRNAs. DNA methylation resets during early embryonic development in mammals (Santos *et al.*, 2002). However, in plants, many DNA methylation sites can be stably transmitted from parents to offspring (Vaughn *et al.*, 2007; Johannes *et al.*, 2008). In asexual dandelions, various factors, including low nutrients, salt stress, jasmonic acid treatment, and salicylic acid treatment, triggered considerable changes in methylation throughout the genome (Verhoeven *et al.*, 2010). A majority of methylation changes, from 74% to 92%, in five treatment groups observed in the first generation were faithfully transmitted to the next generation (Verhoeven *et al.*, 2010). Compared with annual herbaceous plants, the generation time of poplar is too long to allow examination of transmission of methylated loci. Perennial woody plants are constantly exposed to environmental changes, requiring rapid, transient, and/or seasonal responses. Thus long-term stable methylation might play very important roles in the responses to environmental stimuli. Our results showed that only ~15% of *de novo* methylation sites remained at 6 months after exposure to abiotic stress in poplar, implying that only a few stress-responsive methylation sites can affect the regulation of transcription in poplar over the long term.

Previous studies have indicated that the methylation ratio of coding genes is significantly higher than that of miRNA genes (Song *et al.*, 2015). In contrast, in this study, either the ratio of methylation or long-term stable methylation of protein-coding genes was also significantly higher than in miRNA genes. Only conserved miRNA6445a showed long-term methylation in response to abiotic stress, implying that the stability of DNA methylation might be correlated with the conservation of DNA elements. Among 164 SDMRs, the number of SDMRs responsive to different abiotic stresses was significantly different, suggesting the existence of stress-specific long-term methylation patterns. Eight SDMRs representing genes that function in photosynthesis, signal transduction pathways of plant hormones, leaf senescence, and transcriptional regulation were co-methylated under all four abiotic stresses, implying that these genes might be important nodes of DNA methylation regulating transcription in response to abiotic stress. *PsiMIR6445a*, which produces a negative regulator, maintains its methylated status for 6 months, implying that it might enhance the abiotic stress resistance of poplar for new seasonal growth.

Supplementary data

Supplementary data are available at *JXB* online.

Methods S1. Supplementary methods.

Table S1. MS-PCR primer sequences.

Table S2. Primers for 5′-RACE mapping of miRNA cleavage sites.

Table S3. Information on real-time PCR primer sequences.

Table S4. Annotation of DNA methylation-related genes.

Table S5. Primers used in the detection of polymorphic methylation-sensitive loci.

Table S6. Relative DNA methylation level of poplar in response to abiotic stress.

Table S7. Annotation of stress-specific differentially methylated regions.

Table S8. Sequences of miRNA, lncRNA, and host genes.

Table S9. Statistics of stable DNA methylation sites.

Table S10. Long-term methylation patterns of stress-specific differentially methylated regions.

Figure S1. Schematic diagram of improved degradome sequencing libraries.

Figure S2. Annotation of stress-specific differentially methylated regions.

Figure S3. Transcription factors of stress-specific differentially methylated genes

Figure S4. Verification of methylation sites using MS-PCR

Figure S5. An illustration of the structure of *PsilncRNA00268512* interacting with *miR396e-3p* and *miR396-5p*.

Figure S6. Correlation analysis of miRNA gene expression and cleaved transcripts of targets.

Figure S7. DNA methylation pattern of *Psi-MIR472* after 1 month under abiotic stress.

Acknowledgements

This work was supported by grants from Fundamental Research Funds for Central Universities (no. TD2012-01) and the Project of the National Natural Science Foundation of China (nos 31170622, 30872042, and 31400553). We are grateful for the sequence information produced by the US Department of Energy Joint Genome Institute (http://www.jgi.doe.gov) The authors declare that they have no competing interests. DZ conceived and designed the experiments. YS carried out the gene expression analysis and drafted the manuscript. DC performed the DNA and RNA extractions and performed MSAP analyses. MT participated in the statistical analyses. All authors read and approved the final manuscript.

References

Altschul SF, Gish W, Miller W, Myers EW, Lipman DJ. 1990. Basic local alignment search tool. Journal of Molecular Biology **215,** 403–410.

Bhaskara GB, Nguyen TT, Verslues PE. 2012. Unique drought resistance functions of the highly ABA-induced clade A protein phosphatase 2Cs. Plant Physiology **160,** 379–395.

Boyko A, Blevins T, Yao Y, Golubov A, Bilichak A, Ilnytskyy Y, Hollunder J, Meins F Jr, Kovalchuk I. 2010. Transgenerational adaptation of Arabidopsis to stress requires DNA methylation and the function of Dicer-like proteins. PLoS One **5,** e9514.

Boyko A, Kovalchuk I. 2007. Epigenetic control of plant stress response. Environmental and Molecular Mutagenesis **49,** 61–72.

Bracken CP, Gregory PA, Kolesnikoff N, Bert AG, Wang J, Shannon MF, Goodall GJ. 2008. A double negative feedback loop between ZEB1-SIP1 and the microRNA-200 family regulates epithelial–mesenchymal transition. Cancer Research **68,** 7846–7854.

Brzeski J, Jerzmanowski A. 2003. Deficient in DNA methylation 1 (DDM1) defines a novel family of chromatin-remodeling factors. Journal of Biological Chemistry **278,** 823–828.

Cao X, Springer NM, Muszynski MG, Phillips RL, Kaeppler S, Jacobsen SE. 2000. Conserved plant genes with similarity to mammalian *de novo* DNA methyltransferases. Proceedings of the National Academy of Sciences, USA **97,** 4979–4984.

Carthew RW, Sontheimer EJ. 2009. Origins and mechanisms of miRNAs and siRNAs. Cell **136,** 642–655.

Chan SW, Henderson IR, Jacobsen SE. 2005. Gardening the genome: DNA methylation in *Arabidopsis thaliana*. Nature Review Genetics **6,** 351–60.

Chen X. 2010. Small RNAs—secrets and surprises of the genome. The Plant Journal **61,** 941–958.

Choi CS, Sano H. 2007. Abiotic-stress induces demethylation and transcriptional activation of a gene encoding a glycerophosphodiesterase-like protein in tobacco plants. Molecular Genetics and Genomics **277,** 589–600.

Demeulemeester MAC, Van Stallen N, De Proft MP. 1999. Degree of DNA methylation in chicory (*Cichorium intybus* L.): influence of plant age and vernalization. Plant Science **142,** 101–108.

Des Marais DL, Skillern WD, Juenger TE. 2014. Deeply diverged alleles in the *Arabidopsis* AREB1 transcription factor drive genome-wide differences in transcriptional response to the environment. Molecular Biology and Evolution **32,** 956–969.

Dyachenko OV, Zakharchenko NS, Shevchuk TV, Bohnert HJ, Cushman JC, Buryanov YI. 2006. Effect of hypermethylation of CCWGG sequences in DNA of *Mesembryanthemum crystallinum* plants on their adaptation to salt stress. Biochemistry **71,** 461–465.

Eisen MB, Spellman PT, Brown PO, Botstein D. 1998. Cluster analysis and display of genome-wide expression patterns. Proceedings of the National Academy of Sciences, USA **95,** 14863–14868.

Flores K, Wolschin F, Corneveaux JJ, Allen AN, Huentelman MJ, Amdam GV. 2012. Genome-wide association between DNA methylation and alternative splicing in an invertebrate. BMC Genomics **13,** 480.

Gendrel AV, Lippman Z, Yordan C, Colot V, Martienssen RA. 2002. Dependence of heterochromatic histone H3 methylation patterns on the Arabidopsis gene *DDM1*. Science **297,** 1871–1873.

Gong Z, Morales-Ruiz T, Ariza RR, Roldán-Arjona T, David L, Zhu JK. 2002. ROS1, a repressor of transcriptional gene silencing in Arabidopsis, encodes a DNA glycosylase/lyase. Cell **111,** 803–814.

Guttikonda SK, Valliyodan B, Neelakandan AK, *et al*. 2014. Overexpression of AtDREB1D transcription factor improves drought tolerance in soybean. Molecular Biology Reports **41,** 7995–8008.

Herman JG, Graff JR, Myohanen S, Nelkin BD, Baylin SB. 1996. Methylation-specific PCR: a novel PCR assay for methylation status of CpG islands. Proceedings of the National Academy of Sciences, USA **93,** 9821–9826.

Jalali S, Bhartiya D, Lalwani MK, Sivasubbu S, Scaria V. 2013. Systematic transcriptome wide analysis of lncRNA–miRNA interactions. PLoS One **8,** e53823.

Jalali S, Jayaraj GG, Scaria V. 2012. Integrative transcriptome analysis suggest processing of a subset of long non-coding RNAs to small RNAs. Biology Direct **7,** 25.

Johannes F, Colot V, Jansen RC. 2008. Epigenome dynamics: a quantitative genetics perspective. Nature Review Genetics **9,** 883–890.

Johnson M, Zaretskaya I, Raytselis Y, Merezhuk Y, McGinnis S, Madden TL. 2008. NCBI BLAST: a better web interface. Nucleic Acids Research **36,** W5-9.

Kapranov P, Cheng J, Dike S, *et al*. 2007. RNA maps reveal new RNA classes and a possible function for pervasive transcription. Science **316,** 1484–1488.

Krokan HE, Standal R, Slupphaug G. 1997. DNA glycosylases in the base excision repair of DNA. Biochemical Journal **325,** 1–16.

Lafon-Placette C, Faivre-Rampant P, Delaunay A, Street N, Brignolas F, Maury S. 2013. Methylome of DNase I sensitive chromatin in Populus trichocarpa shoot apical meristematic cells: a simplified approach revealing characteristics of gene-body DNA methylation in open chromatin state. New Phytologist **197,** 416–430.

Lee B, Henderson DA, Zhu JK. 2005. The Arabidopsis cold-responsive transcriptome and its regulation by *ICE1*. The Plant Cell **17,** 3155–3175.

Li D, Zhao Y, Liu C, *et al*. 2011. Analysis of MiR-195 and MiR497 expression, regulation and role in breast cancer. Clinical Cancer Reserach **17,** 1722–1730.

Liang D, Zhang Z, Wu H, *et al*. 2014. Single-base-resolution methylomes of *Populus trichocarpa* reveal the association between DNA methylation and drought stress. BMC Genetics **1,** S9.

Lippman Z, Gendrel AV, Black M, Vaughn MW, Dedhia N, McCombie WR. 2004. Role of transposable elements in heterochromatin and epigenetic control. Nature **430,** 471–476.

Livak KJ, Schmittgen TD. 2001. Analysis of relative gene expression data using real-time quantitative PCR and the 2(-Delta Delta C(T)) Method. Methods **25,** 402–8.

Malagnac F, Bartee L, Bender J. 2002. An Arabidopsis SET domain protein required for maintenance but not establishment of DNA methylation. EMBO Journal **21,** 6842–6852.

Molinier J, Ries G, Zipfel C, Hohn B. 2006. Transgeneration memory of stress in plants. Nature **442,** 1046–1049.

Nakamura S, Hosaka K. 2010. DNA methylation in diploid inbred lines of potatoes and its possible role in the regulation of heterosis. Theoretical and Applied Genetics **120,** 205–214.

Peredo EL, Revilla MA, Arroyo-Garcyá R. 2006. Assessment of genetic and epigenetic variation in hop plants regenerated from sequential subcultures of organogenic calli. Journal of Plant Physiology **163,** 1071–1079.

Poliseno L, Salmena L, Zhang J, Carver B, Haveman WJ, Pandolfi PP. 2010. A coding-independent function of gene and pseudogene mRNAs regulates tumour biology. Nature **465,** 1033–1038.

Ponting CP, Oliver PL, Reik W. 2009. Evolution and functions of long noncoding RNAs. Cell **136,** 629–641.

Rinn JL, Chang HY. 2012. Genome regulation by long noncoding RNAs. Annual Review of Biochemistry **81,** 145–166.

Salmena L, Poliseno L, Tay Y, Kats L, Pandolfi PP. 2011. A ceRNA hypothesis: the Rosetta Stone of a hidden RNA language? Cell **146,** 353–358.

Santos F, Hendrich B, Reik W, Dean W. 2002. Dynamic reprogramming of DNA methylation in the early mouse embryo. Development Biology **241,** 172–182.

Saze H, Scheid OM, Paszkowski J. 2003. Maintenance of CpG methylation is essential for epigenetic inheritance during plant gametogenesis. Nature Genetics **34,** 65–69.

Sha AH, Lin XH, Huang JB, Zhang DP. 2005. Analysis of DNA methylation related to rice adult plant resistance to bacterial blight based on methylation-sensitive AFLP. Molecular Genetics and Genomics **273,** 484–490.

Song YP, Ci D, Tian M, Zhang DQ. 2014. Comparison of the physiological effects and transcriptome responses of *Populus simonii* under different abiotic stresses. Plant Molecular Biology **86,** 139–156.

Song YP, Tian M, Ci D, Zhang DQ. 2015. Methylation of microRNA genes regulates gene expression in bisexual flower development in andromonoecious poplar. Journal of Experimental Botany **66,** 1891–1905.

Steward N, Ito M, Yamaguchi Y, Koizumi N, Sano H. 2002. Periodic DNA methylation in maize nucleosomes and demethylation by environmental stress. Journal of Biology Chemistry **277,** 37741–37746.

Suzuki MM, Bird A. 2008. DNA methylation landscapes: provocative insights from epigenomics. Nature Reviews Genetics **9,** 465–476.

Tafer H, Hofacker IL. 2008. RNAplex: a fast tool for RNA–RNA interaction search. Bioinformatics **24,** 2657–63.

Tixier MH, Sourdille RM, Leroy P, Bernard M. 1997. Detection of wheat microsatellites using a non-radioactive silver-nitrate staining method. Journal of Genetics and Breeding **51,** 175–177.

van Bakel H, Nislow C, Blencowe BJ, Hughes TR. 2010. Most 'dark matter' transcripts are associated with known genes. PLoS Biology **8,** e1000371.

Vaughn MW, Tanurdzić M, Lippman Z, *et al*. 2007. Epigenetic natural variation in *Arabidopsis thaliana*. PLoS Biology **5,** 1617–1629.

Verhoeven KJ, Jansen JJ, van Dijk PJ, Biere A. 2010. Stress-induced DNA methylation changes and their heritability in asexual dandelions. New Phytologist **185,** 1108–18.

Vining KJ, Pomraning KR, Wilhelm LJ, Priest HD, Pellegrini M, Mockler TC, Freitag M, Strauss SH. 2012. Dynamic DNA cytosine methylation in the *Populus trichocarpa* genome: tissue-level variation and relationship to gene expression. BMC Genomics **13,** 27.

Voinnet O. 2009. Origin, biogenesis, and activity of plant microRNAs. Cell **136,** 669–687.

Vrba L, Jensen TJ, Garbe JC, Heimark RL, Cress AE, Dickinson S, Stampfer MR, Futscher BW. 2010. Role for DNA methylation in the regulation of miR-200c and miR-141 expression in normal and cancer cells. PLoS One **5,** e8697.

Wang WY, Chen WS, Chen WH, Hung LS, Chang PS. 2002. Influence of abscisic acid on flowering in *Phalaenopsis hybrida*. Plant Physiology and Biochemistry **40,** 97–100.

Wei ZZ, Du QZ, Zhang JF, Li BL, Zhang DQ. 2012. Genetic diversity and population structure in Chinese indigenous poplar (*Populus simonii*) populations using microsatellite markers. Plant Molecular Biology Reporter **31,** 620–632.

Wilusz JE, Sunwoo H, Spector DL. 2009. Long noncoding RNAs: functional surprises from the RNA world. Genes and Devlopment **23,** 1494–1504.

Wu L, Zhou HY, Zhang QQ, *et al*. 2010. DNA methylation mediated by a microRNA pathway. Molecular Cell **38,** 465–475.

Xiao W, Gehring M, Choi Y, Margossian L, Pu H, Harada JJ, Goldberg RB, Pennell RI, Fischer RL. 2003. Imprinting of the MEA Polycomb gene is controlled by antagonism between MET1 methyltransferase and DME glycosylase. *Development* Cell **5,** 891–901.

Xiang H, Zhu J, Chen Q, *et al*. 2010. Single base-resolution methylome of the silkworm reveals a sparse epigenomic map. Nature Biotechnology **28,** 516–520.

Zemach A, McDaniel IE, Silva P, Zilberman D. 2010. Genome-wide evolutionary analysis of eukaryotic DNA methylation. Science **328,** 916–919.

Zhang J, Mujahid H, Hou Y, Nallamilli BR, Peng Z. 2013. Plant long ncRNAs: a new frontier for gene regulatory control. American Journal of Plant Science **4,** 1038–1045.

Zhang X, Yazaki J, Sundaresan A, *et al*. 2006. Genome-wide high-resolution mapping and functional analysis of DNA methylation in Arabidopsis. Cell **126,** 1189–1201.

Zhou S, Sun H, Zheng B, Li R, Zhang W. 2014. Cell cycle transcription factor E2F2 mediates non-stress temperature response of *AtHSP70-4* in Arabidopsis. Biochemical and Biophysical Research Communications **455,** 139–46.

Zhu QH, Wang MB. 2012. Molecular functions of long non-coding RNAs in plants. Genes **3,** 176–190.